Nonlinear Rheology of Wormlike Micelles

N. A. Spenley,[1] M. E. Cates,[1] and T. C. B. McLeish[2]
[1]*Cavendish Laboratory, Madingley Road, Cambridge CB3 0HE, United Kingdom*
[2]*Department of Physics, University of Sheffield, Sheffield S3 7RH, United Kingdom*
(Received 13 January 1993)

Certain viscoelastic surfactant solutions show unusual nonlinear rheology: In steady shear, the shear stress saturates to a constant value while the first normal stress increases roughly linearly with shear rate over several decades. Here we explain this behavior in terms of the "reptation-reaction" model for the dynamics of reversibly breakable, polymerlike micelles. The constitutive equation for this model leads to a flow instability of shear-banding type. The limiting shear stress is predicted to be $\sigma^* = 0.67 G_0$ (with G_0 the plateau modulus), in quantitative agreement with experiment.

PACS numbers: 83.50.Fc, 05.40.+j, 36.20.Ey

In several aqueous surfactant systems, the amphiphilic molecules are known to aggregate reversibly into long, flexible wormlike micelles [1]. These can become entangled leading to viscoelastic phases, which in many respects resemble semidilute polymer solutions. Such phases have particularly interesting flow behavior (rheology), and this has been the subject of extensive theoretical and experimental study in recent years [1–10].

Unlike conventional polymers, micelles are reversibly breakable and this has profound consequences on the mechanism for stress relaxation in these materials [7,8]. A model for the dynamics of entangled micelles has been proposed [7], which invokes the conventional reptation mechanism [11], in which each polymer is viewed as effectively confined to a "tube" from which it can escape only by a snakelike motion. The reptation process is then coupled to a set of reaction equations describing the reversible scission and recombination of chains. The linear response function $G(t)$ for stress relaxation following a small step strain can then be calculated [7–9]. In the fast breaking limit, where scission reactions are frequent on the time scale of reptation, relaxation is predicted to approach a pure Maxwell form, $G(t) = G_0 e^{-t/\tau}$, where G_0 is the plateau modulus and τ a relaxation time of order $(\tau_d \tau_b)^{1/2}$ where τ_d is the time scale for reptation and τ_b that for micellar breakdown [7–9].

The pure Maxwell behavior predicted by the model has been observed, in some cases with an accuracy not matched by any other class of materials [2–5]. The origin of the single relaxation time is a form of motional narrowing: On the (rapid) time scale of breaking, the system forgets all information about the disposition of chain ends with respect to any particular segment of tube. Stress relaxation occurs when a chain end passes through the given tube segment; in the fast reaction limit, the same decay rate governs all tube segments in the system. At very short time scales (of order τ_b) there are departures from the Maxwell form, which can be fitted using the numerical solution of the model [8].

Thus the reptation-reaction model of Ref. [7] seems to account rather well for the observed linear viscoelastic spectrum of entangled micellar solutions. However, the real test of entanglement theories of viscoelasticity lies in the prediction of *nonlinear* behavior; for micelles this can be spectacular in both transient and steady flows [4–6]. Various studies of transient effects have been made, but only recently have detailed results for the steady-shear response of a viscoelastic surfactant solution become available [5]. The nonlinear response of a material is governed by its constitutive relation, which determines the stress at time t in terms of the flow history over earlier times $t' < t$. In what follows we restrict our attention to steady shear for which the flow history is especially simple.

A constitutive scheme for reversibly breakable chains was proposed, but not solved, in Ref. [10]. The stress tensor is written as

$$\mathsf{S} = \tfrac{15}{4} G_0 [\mathsf{W} - \tfrac{1}{3}\mathsf{I}] ,$$

where $\mathsf{W} = \langle \mathbf{uu} \rangle$ is the (tensorial) second moment of the orientational distribution function for tube segments, and I is the unit tensor. For steady flow, the quantity W obeys [10]

$$\mathsf{W}(t) = \int_0^\infty \mathcal{B} \exp[-(t-t')\mathcal{D}(v)] \tilde{\mathbf{Q}}(t-t') dt' . \quad (1)$$

This equation is derived by considering the creation and destruction of stress elements (tube segments). $\mathcal{B} = 1/\tau$ is the rate of creation of new tube segments at times $t' < t$ by reptative motion of chain ends, whereas $\mathcal{D} = 1/\tau + v$ is the death rate, which has contributions both from reptation and from "retraction." Retraction arises because a tube under steady flow is subject to fractional increase in length per unit time $v = \mathsf{W} \cdot \mathsf{K}$, with K the velocity gradient tensor [11]. The chain retracts to maintain constant tube length (the "first relaxation process" of Doi and Edwards [11]), thus losing the tube segments at a rate v. Finally, $\tilde{\mathbf{Q}}(t-t')$ is the stress contributed by an element of tube created at $t' < t$, which has been both rotated and stretched by the flow over the intervening time. This is written as a surface integral over the unit sphere [10]

0031-9007/93/71(6)/939(4)$06.00

$$\tilde{\mathbf{Q}}(\xi)=\frac{1}{4\pi}\int\frac{[\mathbf{E}(\xi)\cdot\mathbf{u}][\mathbf{E}(\xi)\cdot\mathbf{u}]}{|\mathbf{E}(\xi)\cdot\mathbf{u}|}d^2\mathbf{u}\,, \tag{2}$$

where $\mathbf{E}(\xi)=\exp[\mathbf{K}\xi]$ is the deformation tensor over a time interval ξ. For simple shear flow along the x direction with the gradient in y, the velocity gradient is $\mathbf{K}=\dot{\gamma}\hat{\mathbf{e}}_x\hat{\mathbf{e}}_y$.

Equation (1) exploits the fast averaging process (on time scales τ_b) to drop any dependence of the birth and death rates ($\mathcal{B},\mathcal{D}$) on the individual tube segments involved. Therefore the equation is restricted to the fast reaction limit, and to shear rates $\dot{\gamma}$ small compared to τ_b^{-1}. The other main assumptions are that the retraction process is instantaneous, and that there is no direct influence of shear rate on the rate of micellar breakage [10]. Finally, our expressions for the dependence of $\mathcal{B}$ and $\mathcal{D}$ on v are not quite exact [10], but we have checked that our predictions are insensitive to small changes in the forms used.

The shear stress $\sigma=S_{xy}$ is plotted as a function of shear rate in Fig. 1. This shows a maximum in shear stress σ^* at a shear rate $\dot{\gamma}_1$. This maximum can be understood as follows. As a tube segment is subjected to greater and greater shear deformation, the stress in it, as determined by Eq. (2), tends to a constant value. This prevents the total shear stress in the sample from increasing indefinitely with higher shear rate. Meanwhile, the death rate due to retraction does increase without limit, so tube segments are renewed faster, causing σ to fall.

The decreasing shear stress at $\dot{\gamma}>\dot{\gamma}_1$ means that steady shear flow in this region is unstable [12]. However, this behavior cannot persist to infinite shear rates, and eventually there must be an upturn in the shear stress curve at flow rates beyond the range for which the model applies (see dashed curve in Fig. 1). We denote the upper shear rate at which S_{xy} again reaches σ^* as $\dot{\gamma}_2$. Steady Couette flow in the regime $\dot{\gamma}_1\ll\dot{\gamma}\ll\dot{\gamma}_2$ can only be supported if the system forms two or more "shear bands." These are layers of high- and low-shear-rate material (of equal shear stress) which coexist at volume fractions arranged to match the imposed macroscopic shear rate. At the interface(s) between bands, the shear stress and the component of the normal stress perpendicular to the interface are both continuous [12].

In fact, a similar shear-banding instability is predicted in ordinary polymer melts and solutions. Though not yet observed directly (for reasons discussed at the end of the paper) it has been proposed as the origin of the so-called "spurt effect" [12]. The shear stress arising in the shear-banded region could in principle lie anywhere between σ^* and the local minimum of the shear stress curve visible in Fig. 1. In pipe flow, the value of σ is selected by the boundary condition on the normal stress [12]. However, for flow in either a Couette cell or a cone-and-plate apparatus, there is no such selection mechanism; we therefore expect that, as the shear rate is slowly increased, the flow remains stable up to the maximum shear stress σ^* [13]. In this case, the observed shear stress will follow the short-dashed line in Fig. 1, with a horizontal plateau in shear stress at $\sigma=\sigma^*=0.67G_0$. The plateau sets in at shear rate $\dot{\gamma}_1=2.6\tau^{-1}$.

Figure 2 shows the predicted shear stress alongside the recent data of Rehage and Hoffman [5] on an aqueous solution of cetylpyridinium chloride/sodium salicylate (CPyCl/NaSal: 100 mM/60 mM). This system has been very carefully characterized and has a clear Maxwell spectrum in linear response, indicating $\tau_b\ll\tau_d$ as required. The relaxation time $\tau=8.5$ s and the plateau modulus $G_0=31.2$ Pa are independently found from linear response measurements, so there are no free parameters in the fit. The agreement between theory and experiment is clearly excellent. Note that the last few experimental data points in Fig. 2 seem to show an upturn from the plateau, suggesting that the shear rate $\dot{\gamma}_2$ may have been reached. This could be checked by looking for hysteresis in the shear stress (following the lower branch in Fig. 1) as the flow rate is decreased from values above $\dot{\gamma}_2$.

We now consider the behavior of the first normal stress, $N_1=S_{xx}-S_{yy}$. Experimentally, this shows a

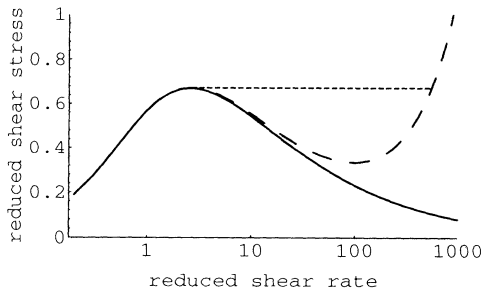

FIG. 1. Log-linear plot of reduced shear stress σ/G_0 against reduced shear rate $\dot{\gamma}\tau$. Long-dashed line: the turnup at high shear. Short-dashed line: the measured shear stress in the unstable region.

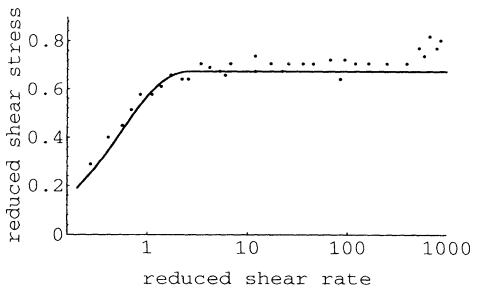

FIG. 2. Log-linear plot of reduced shear stress σ/G_0 against reduced shear rate $\dot{\gamma}\tau$. The solid curve is the prediction of the model with no adjustable parameters. The data are from Ref. [5]. Note the apparent turnup at high shear.

roughly linear increase with shear rate in the shear-banded region (shown in Fig. 3). At the upper end of the range, normal stresses are obtained that are very large compared to those measured for shear rates near $\dot{\gamma}_1$ (where $N_1 \simeq G_0$). The near-linear dependence is quite consistent with the shear-banding mechanism, so long as we adopt a model of the high shear phase (of shear rate $\dot{\gamma}_2$) for which the value of N_1 is indeed very large compared to G_0. Well within the banded region, the normal stress will then increase linearly, in proportion to the volume fraction of high shear material required to maintain the imposed overall flow rate.

To proceed further, we need to model the high shear phase more quantitatively. This is difficult, and necessitates several assumptions beyond those used above. However, for unbreakable chains, a model has recently been proposed which does predict the form of the shear and normal stresses in the very high shear regime [13]. The model involves a chain which at high shear is constrained to lie in a tube aligned along the flow. Conventional tube models neglect any fluctuations in the position of the chain about the axis of the tube, and so predict a monotonically decreasing shear stress [14]. Accounting for the finite extent of the chain transverse to the flow direction, the authors of Ref. [13] obtained the following asymptotic estimates for the stresses at high shear:

$$\sigma \simeq \tfrac{5}{4} G_0 \dot{\gamma} \tau_r N_T^{-2}; \quad N_1 \simeq \tfrac{15}{2} G_0 (\dot{\gamma}\tau_r)^2 N_T^{-2}. \qquad (3)$$

Here N_T is the number of tube segments per chain, and $\tau_r \simeq \tau_d / N_T$ the Rouse time, characteristic of the decay of stretching modes of a chain within its tube (i.e., the first relaxation). These expressions are expected to apply for shear rates $\dot{\gamma} \gg \tau_r^{-1} N_T$; they also assume that the number of statistical segments between entanglements obeys $N_e \geq N_T^2$ [13]. The prefactors quoted above are those for an exponential length distribution [1] rather than monodisperse as considered in Ref. [13]; N_T and τ_r refer to the mean chain length.

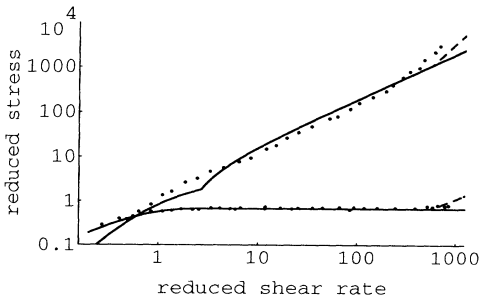

FIG. 3. Log-log plot of reduced shear and normal stresses against reduced shear rate. The solid curves are predictions of the model with $\alpha = 0.53$ (the upper line is normal stress; the lower is shear stress). Dotted curves are obtained by also assuming $N_T = 25$. The points are experimental data from Ref. [5].

We now propose that these asymptotic forms for the stresses apply, even for reversibly breakable chains. This is at least arguable, so long as we assume that the high shear phase corresponds to a regime where $\dot{\gamma} \gg \tau_b^{-1}$. In this case, the fact that the chains are reversibly breakable may have relatively little effect: On the characteristic time scale of chain deformation ($\dot{\gamma}^{-1}$) a chain typically does not break or re-form. With this assumption, we can calculate from Eq. (3) the high shear part of the shear and normal stress curves explicitly, and use the results in a fit to the normal stress data.

As mentioned previously, the data of Ref. [5] show some turnup in shear stress at the highest shear rates. If we set aside this part of the data, the normal stress curve can be used to determine a parameter $\alpha = \tau_r / \tau$, which —crudely speaking—characterizes the average slope of the N_1 curve in the shear-banded region. (In fact, the parameter is extracted by a least squares fit to the entire N_1 data set, excluding the last few points.) The best fit is shown in Fig. 3, resulting in a value of $\alpha \simeq 0.5$. For consistency with Eq. (1)—which assumes instantaneous retraction—this parameter should be small. The value found is marginal, but certainly not inconsistent, bearing in mind that the prefactors in Eq. (3) are at best known only to within order unity factors [13]. It is possible that a more detailed treatment, allowing for non-negligible α would partially smooth out the "kink" visible in the predicted N_1 curve.

The model for the high shear limit also involves a second parameter, which we choose as N_T. This determines the location of $\dot{\gamma}_2$ at which σ starts to rise from its plateau, and N_1 jumps abruptly from a linear to a quadratic dependence on $\dot{\gamma}$. The experimental data at high shear are somewhat ambiguous, but if the apparent turnup in the shear stress (Fig. 2) is a real effect, we must have $\dot{\gamma}_2 \tau \simeq 500$, which then determines $N_T \simeq 25$. (The stresses then predicted for $\dot{\gamma} > \dot{\gamma}_2$ are indicated in Fig. 3.) The result for N_T is in very good agreement with an independent estimate found by analyzing the shape of the linear viscoelastic spectrum at high frequencies [9]. If instead the apparent turnup is an artifact, then $\dot{\gamma}_2$ must still be greater than about 500, which implies $N_T \geq 25$.

If we accept the (tentative) idea that the reversible breakage of chains is irrelevant at high enough shear rates, then the consistency of our estimates for the parameters α and N_T offers strong support for the model of Ref. [13] for the high shear limit of unbreakable polymers. It is instructive to compare also with other models; for example, fits can also be made on the assumption that the high shear branch of the stress curves follow the Rouse model, which describes unentangled, unbreakable chains [11]. This gives a less consistent value of α (somewhat larger than unity), and a value of $N_T = 800$, which is unfeasibly large compared to that extracted from the linear response spectrum [9].

In summary, we have shown that the nonlinear viscoelastic behavior of an entangled micellar solution under

steady shear [5] is fully consistent with a constitutive equation based on the "reptation-reaction" model of the dynamics of wormlike micelles [10]. The nonlinear behavior is dominated by a flow instability of shear-banding type, which sets in at a shear rate $\dot{\gamma}_1 \simeq \tau^{-1}$ where τ is the Maxwell time of the fluid. This is the first direct evidence for this type of instability in entangled liquids: By assuming its existence, we can account for the experimental results on micelles with convincing accuracy. Of course, many open questions remain, for example, concerning transient phenomena (startup flows) as well as the details of the behavior at very high shear.

As mentioned earlier, for conventional (unbreakable) polymers, the Doi-Edwards theory [11] predicts a shear stress which qualitatively resembles the solid curve in Fig. 1 for micelles. Accounting also for a turnup in the stress at high shear rate (see, e.g., [13]), we expect conventional polymers to show a similar plateau region in shear stress resulting from the same type of flow instability. However, this has not yet been observed, perhaps in part because of practical difficulties in studying polymers at high shear rates. For example, in cone-and-plate work on polymer melts, the sample is often expelled from the rheometer. As discussed in Ref. [13], this normal stress phenomenon may be overcome by studying highly entangled systems of relatively low elastic modulus, of which viscoelastic micellar phases are a prime example. The presence in micellar systems of a single relaxation time also favors observation of the instability: For conventional polymers, the shear stress maximum could be smeared out by polydispersity effects [12]. Finally, micellar systems are not subject to the risk of irreversible sample degregation which always attends work on conventional polymers at very high flow rates. For these reasons, we believe that micellar systems provide an important tool for studying the effects of entanglements in flow regions not easily accessible using conventional polymers.

We are grateful to G. Marrucci, H. Rehage, and S. J. Candau for valuable discussions. N.A.S. thanks the Science and Engineering Research Council (U.K.) and Shell Research Limited, Thornton Research Centre for receipt of a CASE award. This work was funded in part under EC Grant No. SCI-0288-C.

[1] For a review, see M. E. Cates and S. J. Candau, J. Phys. Condens. Matter **2**, 6869 (1990).
[2] G. Porte and J. Appell, J. Phys. Chem. **85**, 2511 (1981); S. J. Candau, E. Hirsch, and R. Zana, J. Colloid Interface Sci. **105**, 521 (1985); F. Kern, R. Zana, and S. J. Candau, Langmuir **7**, 1344 (1991).
[3] T. Shikata, H. Hirata, and T. Kotaka, Langmuir **3**, 1081 (1987); **4**, 354 (1988).
[4] H. Hoffmann, H. Loebl, H. Rehage, and I. Wunderlich, Tenside Deterg. **22**, 290 (1985); I. Wunderlich, H. Hoffmann, and H. Rehage, Rheol. Acta **26**, 532 (1987); H. Rehage and H. Hoffmann, J. Phys. Chem. **92**, 4217 (1988).
[5] H. Rehage and H. Hoffmann, Mol. Phys. **74**, 933 (1991).
[6] T. Shikata, H. Hirata, E. Takatori, and K. Osaki, J. Non-Newtonian Fluid Mech. **28**, 171 (1988).
[7] M. E. Cates, Macromolecules **20**, 2289 (1987).
[8] M. S. Turner and M. E. Cates, Langmuir **7**, 1590 (1991).
[9] R. Granek and M. E. Cates, J. Chem. Phys. **96**, 4758 (1992).
[10] M. E. Cates, J. Phys. Chem. **94**, 371 (1990).
[11] M. Doi and S. F. Edwards, *The Theory of Polymer Dynamics* (Clarendon, Oxford, 1986).
[12] T. C. B. McLeish and R. C. Ball, J. Polym. Sci. Polym. Phys. Edn. **24**, 1735 (1986); T. C. B. McLeish, J. Polym. Sci. Polym. Phys. Edn. **25**, 2253 (1987), and references therein.
[13] M. E. Cates, T. C. B. McLeish, and G. Marrucci, Europhys. Lett. **21**, 451 (1993).
[14] G. Marrucci and N. Grizzuti, Gazz. Chim. Ital. **188**, 179 (1988).